

Modulation of PKC signaling and induction of apoptosis through suppression of reactive oxygen species and tumor necrosis factor receptor 1 (TNFR1): key role of quercetin in cancer prevention

Akhilendra Kumar Maurya¹ · Manjula Vinayak¹

Received: 16 April 2015 / Accepted: 1 June 2015 / Published online: 16 June 2015
© International Society of Oncology and BioMarkers (ISOBM) 2015

Abstract Cancer cells are characterized by increased production of reactive oxygen species (ROS) and an altered redox environment as compared to normal cells. Continuous accumulation of ROS triggers oxidative stress leading to hyperactivation of signaling pathways that promote cell proliferation, survival, and metabolic adaptation to the tumor microenvironment. Therefore, antioxidants are proposed to contribute to cancer prevention. Protein kinase C (PKC) is a crucial regulator of diverse cellular processes and contributes to cancer progression. The activation of PKC is partially dependent on ROS signaling. In the present study, cancer preventive activity of natural flavonoid quercetin is analyzed in ascite cells of Dalton's lymphoma-bearing mice. The total ROS level and activity of PKC were downregulated after quercetin treatment in lymphoma-bearing mice. Quercetin modulates the expression of almost all isozymes of classical, novel, and atypical PKC as well as downregulates the level and expression of PKC α . Further, quercetin improves apoptotic potential, as observed by the levels of caspase 3, caspase 9, PARP, PKC δ , and nuclear condensation. Additionally, quercetin reduces cell survival and promotes death receptor-mediated apoptosis via differential localization of the TNFR1 level in ascite cells. The overall result suggests the cancer preventive activity of quercetin via the induction of apoptosis and modulates PKC signaling with the reduction of oxidative stress in ascite cells of lymphoma-bearing mice.

Keywords ROS · PKC · Apoptosis · Quercetin · TNFR1 and Dalton's lymphoma

Introduction

Cells are constantly generating reactive oxygen species (ROS) during aerobic metabolism. Each cell is equipped with an extensive antioxidant defense system to combat excessive production of ROS. Oxidative stress exists in cells when the generation of ROS overcomes the cell's natural antioxidant defense [1, 2]. Excessive ROS may be generated as a result of elevated metabolic processes or from toxic insult. A high level of ROS directly induces oxidative damage in lipids, proteins, and nucleic acids [3]. There is a growing consensus that oxidative stress contributes to the initiation of cellular malignancy and progression of cancer owing to genomic instability, especially due to mutations in proto-oncogenes and tumor suppressor genes, and subsequent activation of signal transduction pathways [2, 4–9]. ROS is considered as a modulator of signaling pathways mediated through extracellular signal-regulated kinases (ERKs), mitogen-activated protein kinases (MAPKs), hypoxia-inducible factors (HIFs), phosphoinositide 3-kinases (PI3Ks), protein kinase C (PKC), etc. to take part in carcinogenesis [5, 7, 10–12]. Cancer cells are dependent on maintaining a high level of ROS that allows pro-tumorigenic cell signaling. The dependency of cancer cells on ROS homeostasis may be potentially exploited to target them therapeutically by modulation of antioxidant enzymes such as superoxide dismutase, catalase, glutathione peroxidase, etc. and non-enzymic antioxidants like ascorbate, tocopherols, tocotrienols, carotenoids, natural flavonoids, melatonin, etc. [1, 13–15].

✉ Manjula Vinayak
manjulavinayak@rediffmail.com
Akhilendra Kumar Maurya
akhilendra28bhu@gmail.com

¹ Biochemistry & Molecular Biology Laboratory, Centre of Advanced Study in Zoology, Banaras Hindu University, Varanasi 221005, India

PKC is a housekeeping enzyme; however, under oxidative stress, it promotes tumorigenesis and malignancy [16, 17]. PKC contains multiple cysteine residue that is oxidatively activated by ROS [10, 18]. The activation of PKC is a prerequisite for NADPH oxidase-dependent ROS generation [19, 20]. Regulatory as well as catalytic domains of PKC are differentially activated which regulate different downstream pathways. Oxidation at the NH₂-terminal regulatory domain activates PKC, whereas oxidation at the COOH terminal inactivates PKC [10]. The isoforms of PKC are divided into three categories, namely classical, novel, and atypical. Different isoenzymes of PKC may exert similar or opposite cellular effects by differential coupling to signaling pathways [21]. Upregulation of PKC α is correlated with an increased cell proliferation in various cancers including lymphoma [22–25].

PKC δ is a ubiquitously expressed and multifunctional kinase implicated in the regulation of cell death [26, 27]. Different apoptotic stimuli have been shown to induce caspase-3-dependant cleavage of PKC δ , resulting in the generation of a constitutively active catalytic fragment which has been implicated in its pro-apoptotic function [28–30].

Cellular toxicity induces the intrinsic pathway of apoptosis via caspase 9 signaling. The extrinsic pathway involves TNFR1 leading to the caspase 8 signaling cascade as well as the activation of nuclear factor kappa-B (NF- κ B) which control a large number of inflammatory genes [31–35].

Lymphoma is a cancer of the lymphatic system that originates from lymphocytes. Dalton's lymphoma is a fast-growing, transplantable murine T cell lymphoma. Flavonoids are known to possess antiproliferative and antitumor activities [36]. Quercetin (QUE) is the active component of dietary flavonoid found in fruits and vegetables. The onion is the richest source of QUE. QUE possesses several biological activities, especially useful in cancer treatment. It is widely used as a nutritional supplement due to antioxidant and anti-inflammatory properties. Approximately 25–50 mg of QUE is estimated to be consumed from the daily diet [37].

Normally, the generation of ROS is balanced by the endogenous antioxidant defense system as well as by exogenous natural antioxidant support. However, since oxidative stress is caused by excess ROS accumulation as compared to antioxidant defense, the administered antioxidant should be useful to scavenge ROS and help to reduce oxidative stress. The present work is aimed to explore the possibility of using QUE, a putative regulator of oxidative stress in the prevention of a lymphoma. The objective of the work is to investigate the effect of QUE on PKC isozymes especially PKC α /PKC δ , its role in the modulation of ROS and regulation of apoptosis in Dalton's lymphoma (DL)-bearing mice.

Materials and methods

Chemicals and antibodies

All chemicals used were of molecular biology and analytical grade. Quercetin, 2', 7'-dichlorofluorescein diacetate (H₂DCFDA), tri-reagents for RNA isolation, and horseradish peroxidase (HRP) conjugated β -actin were purchased from Sigma-Aldrich (St. Louis, MO); anti-rabbit caspase 3 and PARP from Cell Signaling Technology (Danvers, MA); anti-rabbit TNFR1 and Caspase 9 assay kit from Biovision (Milpitas, CA); anti-rabbit PKC α from Santa Cruz (Dallas, TX); HRP-conjugated goat anti-rabbit secondary antibody from Bangalore Genei (Bangalore, India); enhanced chemiluminescence (ECL) Super Signal Kit from Pierce Biotechnology (Rockford, IL); PKC assay kit from Promega (Madison, WI); cDNA synthesis kit and 100 bp Plus DNA ladder from Thermo Scientific (Waltham, MA), and ethidium bromide and acridine orange from Loba Chemie (Mumbai, India).

Animals and induction of murine T cell lymphoma (Dalton's lymphoma)

AKR strain mice were bred and maintained under standard laboratory conditions with proper human care, as per the guidelines of the Institutional Animal Ethical Committee, Banaras Hindu University, Varanasi, at 25 \pm 2 °C under a 12-h light/12-h dark schedule with standard mice feed and drinking water ad libitum. Healthy adult male mice (16–20 weeks old and 30 \pm 2 g) were used in the experimental work. About 1 \times 10⁶ viable DL ascite cells in 1 ml of PBS per mouse were transplanted to adult male mice intraperitoneally (i.p.) as described earlier [36]. The success rate of DL development is 100 %. DL ascite cells were a gift from Professor Ajit Sodhi, School of Biotechnology, Banaras Hindu University, Varanasi, India. Dalton's lymphoma is a transplantable murine T cell lymphoma originated in the thymus gland of a DBA/2 mouse at the National Cancer Institute, Bethesda, MD, in 1947 [38].

Schedule of QUE treatment to DL mice and sample collection

The development of DL was confirmed by abnormal abdominal swelling and increased body weight due to accumulation of ascite cells, which were visible clearly on 10–11 days post transplantation. Based on the observation, the first 7–9 days of DL cell growth may be compared with the lag phase/preparatory phase of the sigmoid curve for ascite cell population growth, followed by the log phase. Therefore, the schedule of QUE treatment to DL mice was selected for 12 days starting from the next day after DL transplantation.

DL mice were randomly divided into four groups with six mice in each group ($n=6$). DMSO is one of the most common

solvents used experimentally to dissolve QUE for in vivo and in vitro purposes. A 0.2 % v/w dose of DMSO is given to mice which is considered to be a non-toxic and safe dose [39]. One group of DL mice received 50 μ l DMSO as vehicle. The other three groups were treated with different doses of QUE by i.p. injection: 25 mg QUE/kg BW (DLT25), 50 mg QUE/kg BW (DLT50), and 75 mg QUE/kg BW (DLT75), dissolved in 50 μ l of DMSO to each mouse per day for 12 days consecutively, starting from the next day after DL transplantation. Mice from each group were sacrificed on the 18th day of post DL transplantation by cervical dislocation. Ascite fluid was taken immediately and preserved at -80°C for further study.

Western blotting

Cells were lysed in buffer containing 20 mM Tris-HCl (pH 7.4), 150 mM NaCl, 1 mM EDTA, 1 mM EGTA, 1 % Triton X-100, and 1 mM PMSF as described previously [36]. Cellular debris was spun down at 14,000g for 20 min at 4°C , and the supernatant was used as whole protein extract. Isolated protein was quantified using Bradford reagent. An equal amount of protein from each sample was separated using 10 % SDS-PAGE and transferred to a PVDF membrane overnight at 4°C . The membrane was blocked in 5 % non-fat milk in PBS (pH 7.4) for 2 h at RT. The membrane was probed separately with primary antibodies PKC α (1:500 dilution, Santa Cruz, Dallas, TX), PKC δ (1:500 dilution, Sigma-Aldrich, St. Louis, MO), caspase 3 (1:1000 dilution, Cell Signaling Technology, Danvers, MA), PARP (1:1000 dilution, Cell Signaling Technology, Danvers, MA), and TNFR1 (1:500 dilution, Biovision, Milpitas, CA) in 1 % BSA and 0.05 % Tween-20 in PBS (PBST; pH 7.4) overnight at 4°C . After thorough washing in $1\times$ PBS for 3 min, the blot was incubated with HRP-conjugated goat anti-rabbit immunoglobulin G (IgG) containing 5 % non-fat milk and 0.05 % Tween-20 in PBST (pH 7.4) for 2 h at RT. Immunoreactive protein was detected using the ECL Super Signal Kit (Pierce Biotechnology) on X-ray film. The intensity of the bands was analyzed by densitometric scanning using the Gel Doc System (Alpha Innotech^{EC}). Relative densitometric values were calculated after normalization with β -actin.

Total RNA isolation and semiquantitative RT-PCR

Expressions of PKC isozymes (PKC α , β , γ , δ , η , ϵ , ζ , and ι genes) were studied by semiquantitative RT-PCR as described previously [36]. Total RNA from each group was isolated separately using TRI-reagent (Sigma-Aldrich) as per the manufacturer's instruction. Total RNA was treated with DNase using TURBO DNA-FreeTM Kit I (DNase I, Ambion) and was converted to cDNA using M-MuLV reverse transcriptase (Revert AidTM, Fermentas Life Science) according to the standard protocol of Fermentas Life Science. Amplification

was performed in a DNA Thermal Cycler (Applied Biosystems) with the gene-specific primers (Table 1). The band intensity of amplified products was visualized in 2 % agarose gel, photographed and analyzed using the Gel Doc System (Alpha Innotech^{EC}). Relative densitometric values were calculated after normalization with β -actin.

Assay of PKC activity

Cells were washed with PBS and lysed in lysis buffer containing 25 mM Tris-HCl (pH 7.4), 0.5 mM EGTA, 0.5 mM EDTA, 0.05 % Triton X-100, 10 mM β -mercaptoethanol, 2 mM phenylmethanesulfonyl fluoride (PMSF), and 10 mg/l leupeptin (pH 7.5). The lysate was centrifuged at 14,000g for 5 min at 4°C and the supernatant was collected as described previously [22]. The total PKC activity was measured using a PepTag non-radioactive assay kit (Promega) according to the manufacturer's protocol.

Localization assay of PKC α and TNFR1

Protein was isolated from a different fraction of ascite cells as per method of Chen N [40]. Ascite cells were lysed in 200 μ l homogenization buffer A (20 mM Tris-HCl pH 8.0, 10 mM EGTA, 2 mM EDTA, 2 mM dithiothreitol, 1 mM phenylmethylsulfonyl fluoride, 25 mg/ml aprotinin, and 10 mg/ml leupeptin). The suspension was sonicated for 10 s with a sonicator and centrifuged at 100,000g for 1 h at 4°C . The supernatant was collected as cytosol fraction. The pellet was resuspended in 200 μ l of homogenization buffer B (1 % Triton X-100 in buffer A) and sonicated for 10 s. The suspension was centrifuged at 15,000g for 15 min at 4°C , and the supernatant was collected as a membrane fraction. The protein concentration of each sample was determined.

Activity of caspase 9

Caspase 9 activity was measured using a Colorimetric Assay Kit (BioVision) according to the manufacturer's protocol. Cells were collected and washed with PBS and resuspended in 25 mM HEPES (pH 7.5), 5 mM MgCl₂, 5 mM EDTA, 5 mM dithiothreitol (DTT), 2 mM PMSF, 10 mg/ml pepstatin A, and 10 mg/ml leupeptin. Cell lysate was clarified by centrifugation at 10,000g for 1 min. Supernatant containing 200 μ g of protein was incubated with 4 mM LEHD-pNA substrate at 30°C for 2 h. Levels of released pNA were measured at 405 nm in a microtiter plate reader (ECIL).

Total ROS measurements

The total ROS level was determined by the oxidative conversion of non-fluorescent 2', 7'-dichlorofluorescein diacetate (H₂DCFDA) to highly fluorescent 2', 7'-dichlorofluorescein

Table 1 Primer pairs and conditions of PCR

Genes	Sequences of primer pairs (F, forward; R, reverse)	PCR condition (annealing)	No. of cycles	Amplicon size (bp)
PKC α	F: 5'-GGTTTGGGAAACAAGGCTTC-3' R: 5'-GCAGAGGCTAGGGACATTGA-3'	58 °C, 40 s	28	278
PKC β	F: 5'-CATCTGGGATGGGGTGACAACC-3' R: 5'-CGGTCGAAGTTTTTCAGCGTTTC-3'	57 °C, 40 s	33	420
PKC γ	F: 5'-GTTCCGTCTGCACAGCTACA-3' R: 5'-CATTGGGGTCCATAGGAATG-3'	56 °C, 40 s	35	263
PKC δ	F: 5'-AGGCCGTGTTATCCAGATTG-3' R: 5'-CGGCCGATAATCTTGTCAAT-3'	58 °C, 40 s	27	426
PKC η	F: 5'-CAAACGCGGGGTGAATG-3' R: 5'-TCCGTTTCACAACTCCATGA-3'	54 °C, 30 s	27	437
PKC ϵ	F: 5'-ACGAGTGTTTCAGGGAGCGTA-3' R: 5'-CGTGGGGACCTTGTAGTTGT-3'	58 °C, 45 s	27	331
PKC ζ	F: 5'-TCAAGTGGGTGGACAGTGAA-3' R: 5'-CCATATCCTTTCGCTGCACT-3'	57 °C, 45 s	30	284
PKC ι	F: 5'-GGGACTTTGCAGTGAGGTTTC-3' R: 5'-CGCTCTGGTACACATGGAAA-3'	56 °C, 40 s	28	192
β -actin	F: 5'-GTGGGCCGCCCTAGGCACCAG-3' R: 5'-TCTTTGATGTCACGCACGATTC-3'	60 °C, 45 s	26	539

(DCF) as described previously [41]. An equal number of cells was used for ROS measurement. Briefly, treated cells were collected and washed two times with PBS. Further, cells were incubated with 10 μ M H₂DCFDA for 30 min in the dark at 37 °C and the intensity of fluorescence was recorded using a 485/530-nm excitation/emission filter. The total ROS level was determined in terms of fluorescence unit per milliliter.

For microscopic detection of ROS production, cells were washed with PBS and incubated in a DMEM medium containing H₂DCFDA (20 μ M) for 30 min at 37 °C and 5 % CO₂. The excess of dye was removed by washing with PBS. ROS production was visualized on an inverted fluorescent microscope (Leica) using a 485/530-nm excitation/emission filter.

Staining with ethidium bromide/acridine orange

To determine apoptosis, ascite cells from DL mice at density 2.5×10^4 cells/well were plated into 96-well plates as described previously [42]. Ethidium bromide/acridine orange mix dye (8 μ l) from the stock solution (100 μ g/ml ethidium bromide and 100 μ g/ml acridine orange in PBS) was added and washed two times with PBS. Cells were viewed under an inverted fluorescence microscope (Leica) at $\times 400$ magnification. Tests were done in triplicate, counting a minimum of 100 cells.

Statistical analysis

All experiments were repeated three times independently, and one representative image is presented in the figures. One-way analysis of variance (ANOVA) followed by the Tukey test was

used for statistical analysis. Data represent the mean \pm S.E.M. *, **, and *** denote significant differences at the level of $p < 0.05$, $p < 0.01$, and $p < 0.001$ respectively, between the DL and QUE-treated DL groups.

Results

QUE decreases the total ROS level

An elevated level of ROS has been observed in different types of cancer including Dalton's lymphoma, which results in oxidative stress [43]. Therefore, the effect of QUE on the ROS level was analyzed using green fluorescence dye H₂DCFDA. Results obtained from fluorescence images show gradual downregulation of the green fluorescence intensity after QUE treatment, suggesting regression of the ROS level in ascite cells [Fig. 1a]. Further, the total ROS level in the ascite cell lysate was studied in terms of fluorescence unit per milliliter using a spectrofluorometer. The total ROS level was significantly downregulated following a similar pattern as found by the fluorescence image. QUE treatment decreases the total ROS level by approximately 88, 82, and 92 % with a dose of 25, 50, and 75 mg/kg BW respectively [Fig. 1b].

QUE inhibits protein kinase C activity

The total PKC activity was found to be decreased in QUE-treated DL mice as compared to DL mice. All the three doses of QUE suppressed PKC activity significantly, approximately by 17.7, 28.6, and 51.1 % with a dose

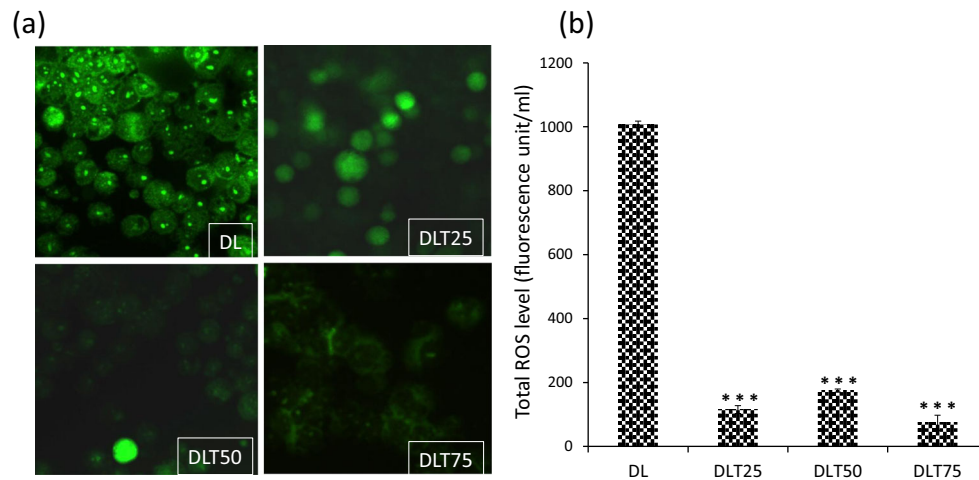


Fig. 1 Total ROS level. Effect of QUE on total ROS level in ascite cells of lymphoma-bearing mice. **a** Fluorescence image of ascite cells by H₂DCFDA staining. **b** Total ROS level in homogenate of ascite cells. Ascite cells of all six animals of each group were pooled separately and used for total ROS measurement. QUE is quercetin and BW is body weight. DL, DLT25, DLT50, and DLT75 represent Dalton's lymphoma-

bearing group and Dalton's lymphoma-bearing group treated with 25, 50, and 75 mg QUE/kg BW respectively. One-way analysis of variance (ANOVA) followed by Tukey test was used for statistical analysis. Data represent the mean±S.E.M. of three independent experiments. *** denotes significant differences at the level of $p < 0.001$, between the DL and QUE treated DL groups

of 25, 50, and 75 mg QUE/kg BW respectively [Fig. 2]. The most significant reduction was found by 75 mg QUE/kg BW.

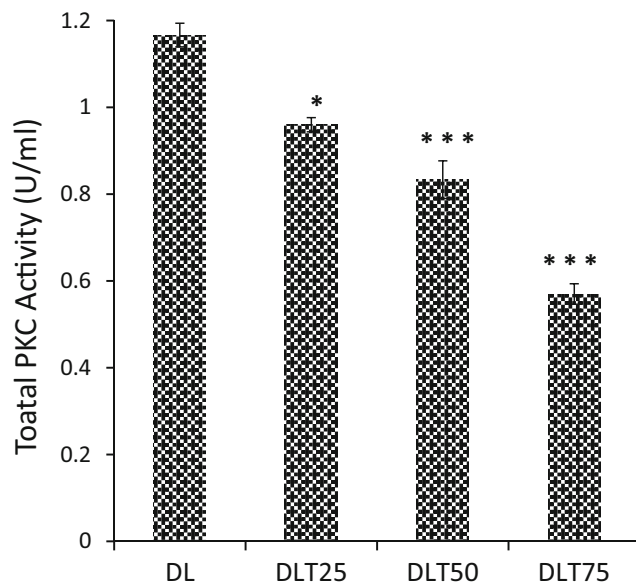


Fig. 2 Total PKC activity. Effect of QUE on total PKC activity in ascite cells of lymphoma-bearing mice. Ascite cells of all six animals of each group were pooled separately, and homogenate was prepared for determination of total PKC activity. QUE is quercetin and BW is body weight. DL, DLT25, DLT50, and DLT75 represent Dalton's lymphoma-bearing group and Dalton's lymphoma-bearing group treated with 25, 50, and 75 mg QUE/kg BW respectively. One-way analysis of variance (ANOVA) followed by Tukey test was used for statistical analysis. Data represent the mean±S.E.M. of three independent experiments. * and *** denotes significant differences at the level of $p < 0.05$ and $p < 0.001$ respectively, between the DL and QUE treated DL groups

Protein level of PKC α

The level of PKC α was examined in the total protein lysate of DL and QUE-treated DL mice by Western blot analysis with an immunospecific PKC α antibody. All doses of QUE significantly downregulated the protein level of PKC α , approximately by 15, 16, and 36 % with a dose of 25, 50, and 75 mg QUE/kg BW respectively in ascite cells [Fig. 3a].

Subcellular localization of PKC α

Subcellular localization of PKC α by Western blotting provides information about the activity of PKC α . One measure of PKC activation is redistribution of PKC α from the cytosolic fraction to a membrane fraction. Therefore, the response of QUE was investigated by monitoring the changes in the distribution patterns of PKC α . Ascite cells were fractionated into the membrane fraction followed by immunoblot analysis for the PKC α . Densitometric scanning of PKC α bands revealed that the level of immune-reactive membrane-associated PKC α is decreased with QUE treatment. QUE downregulates the PKC α approximately by 19, 36, and 43 % in the membrane fraction of ascite cells with a dose of 25, 50, and 75 mg QUE/kg BW respectively [Fig. 3b].

Protein level of PKC δ

PKC δ is known to be a pro-apoptotic protein and its decreased level has been reported in many cancers. PKC δ promotes caspase-3-dependent apoptosis by the cleavage fragment (CF) of PKC δ in Dalton's lymphoma [44]. Therefore, the

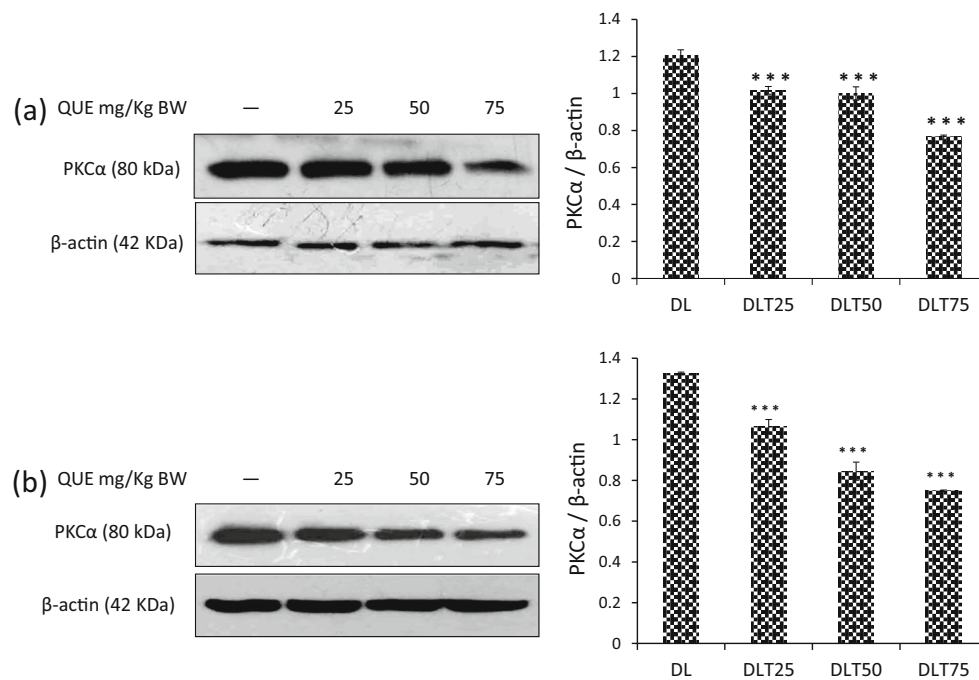


Fig. 3 Level of PKC α . Effect of QUE on protein level and localization of PKC α in ascite cells of lymphoma-bearing mice. Western analysis of PKC α in **a** total protein lysate, **b** membrane fraction, and densitometric scanning of PKC α after normalization with β -actin. Ascite cells of all six animals of each group were pooled separately, and homogenate was prepared for Western analysis of PKC α . *QUE* is quercetin and *BW* is body weight. DL, DLT25, DLT50, and DLT75 represent Dalton's

lymphoma-bearing group and Dalton's lymphoma-bearing group treated with 25, 50, and 75 mg QUE/kg BW respectively. One-way analysis of variance (ANOVA) followed by Tukey test was used for statistical analysis. Data represent the mean \pm S.E.M. of three independent experiments. *** denotes significant differences at the level of $p < 0.001$, between the DL and QUE treated DL groups

effect of QUE on the protein level of PKC δ was analyzed by Western blotting. QUE treatment upregulates the cleavage fragment (CF) of PKC δ , approximately by 2.02- and 2.34-fold with a dose of 50 and 75 mg QUE/kg BW respectively, which supports the pro-apoptotic activity of QUE in DL mice. Twenty-five milligrams of QUE per kilogram BW did not show any upregulation of PKC δ [Fig. 4].

QUE decreases the level of TNFR1

Biological effects of TNF- α are exerted through binding to TNF- α receptor 1 (TNFR1), a 55-kDa protein. To explore the presence of TNFR1 and effect of QUE on TNFR1 in ascite cells, Western blot analysis was done in whole-cell extracts. The result shows that QUE significantly downregulates the

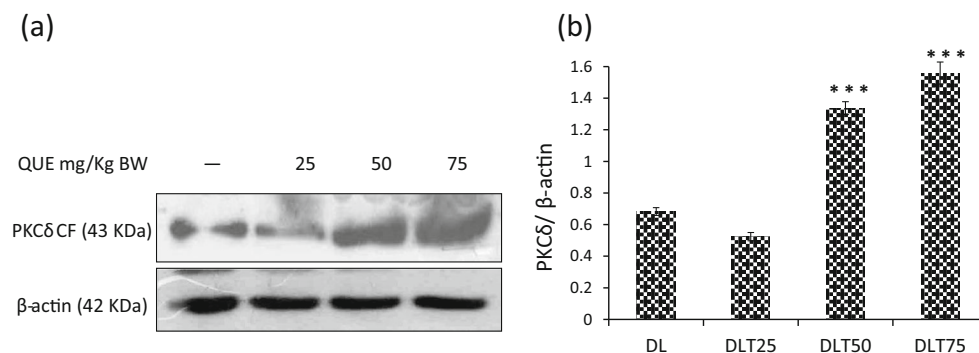


Fig. 4 Level of PKC δ . Effect of QUE on protein level of cleavage fragment (CF) of PKC δ in ascite cells of lymphoma-bearing mice. **a** Western analysis of PKC δ and β -actin. **b** Densitometric scanning of PKC δ after normalization with β -actin. Ascite cells of all six animals of each group were pooled separately, and homogenate was prepared for Western analysis of PKC δ . *QUE* is quercetin and *BW* is body weight. DL, DLT25, DLT50, and DLT75 represent Dalton's lymphoma-bearing

group and Dalton's lymphoma-bearing group treated with 25, 50, and 75 mg QUE/kg BW respectively. One-way analysis of variance (ANOVA) followed by Tukey test was used for statistical analysis. Data represent the mean \pm S.E.M. of three independent experiments. *** denotes significant differences at the level of $p < 0.001$, between the DL and QUE treated DL groups

protein level of TNFR1 in a dose-dependent manner, approximately by 17, 42, and 63 % with a dose of 25, 50, and 75 mg QUE/kg BW respectively [Fig. 5a].

Subcellular localization of TNFR1

Subcellular localization of TNFR1 by Western blotting provides information about differential functions of TNFR1 in ascite cells. Therefore, a change in the distribution pattern of TNFR1 was compared in DL and QUE-treated DL mice. Ascite cells were fractionated into cytosolic and membrane fractions followed by immunoblot analysis for TNFR1. QUE treatment increased the TNFR1 level in the cytosolic fraction in a dose-dependent manner indicating increased apoptosis, whereas it is decreased in the membrane fraction indicating reduced survival. The TNFR1 level is significantly decreased approximately by 28, 40, and 52 % in the membrane fraction, whereas the level of TNFR1 in the cytosolic fraction was found increased by 35, 46, and 73 % with a dose of 25, 50, and 75 mg QUE/kg BW respectively [Fig. 5b, c].

QUE induces apoptosis

Apart from cell proliferation, apoptosis is a hallmark to assess the overall growth of cancer. An increase in apoptosis is correlated with the suppression of cancer growth.

Fluorescence microscopy with differential uptake of fluorescent DNA binding dyes such as ethidium bromide (EB)/acridine orange (AO) staining is a method of choice for its simplicity, rapidity, and accuracy [42, 45]. EB/AO-stained nuclei are classified into (a) viable cells having uniformly green nuclei with a highly organized structure, (b) early apoptotic cells having green nuclei with perinuclear chromatin condensation visible as bright green patches or fragments, (c) late apoptotic cells having orange to red nuclei with condensed or fragmented chromatin, and (d) necrotic cells, swollen to large sizes with uniform orange to red fluorescing nuclei. QUE treatment gradually increases apoptotic cell death in comparison to necrosis [Fig. 6]. Morphological changes indicate that ascite cells follow apoptotic cell death.

Caspase and PARP are key players of apoptosis. Therefore, we have analyzed the effect of QUE on caspase 9, caspase 3, and PARP level. The level of procaspase 3 is decreased with increasing QUE dose, while the active caspase 3 level is found enhanced with increasing dose of QUE [Fig. 7a]. Similarly, significantly improved activity of caspase 9 is observed after QUE treatment in DL mice [Fig. 7c]. Caspase 3 is a critical executioner of apoptosis. It is either partially or totally responsible for proteolytic cleavage of poly (ADP-ribose) polymerase (PARP). The result shows downregulation of full-length PARP with QUE treatment, while the cleaved PARP level was maximally observed with 75 mg QUE/kg BW [Fig. 7a].

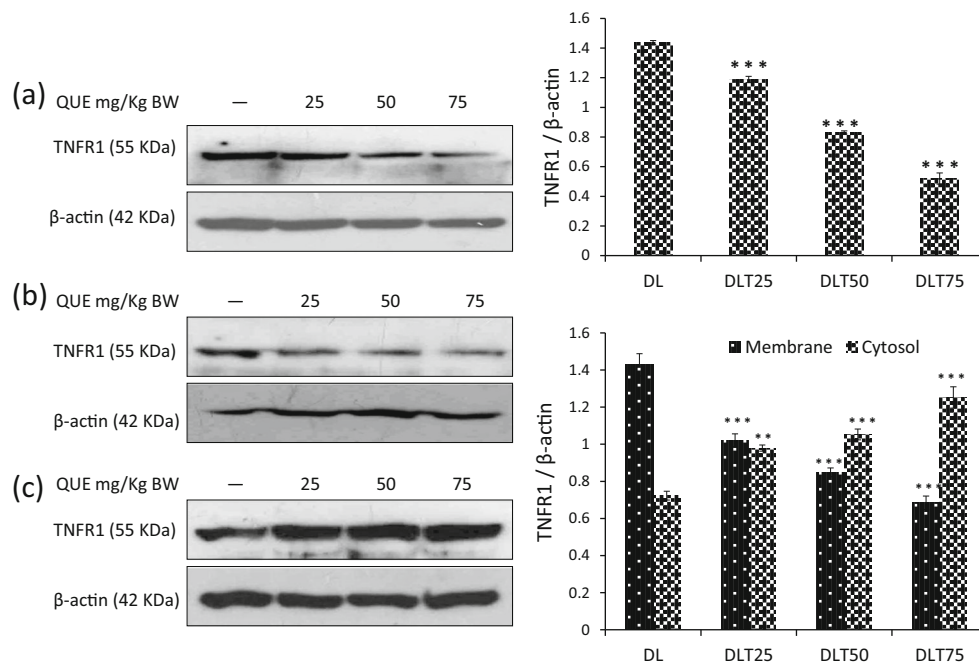


Fig. 5 Level and localization of TNFR1. Effect of QUE on protein level and localization of TNFR1 in ascite cells of lymphoma-bearing mice. Western analysis of TNFR1 and densitometric scanning of TNFR1 after normalization with β -actin in **a** total protein lysate, **b** membrane fraction, and **c** cytosolic fraction. Ascite cells of all six animals of each group were pooled separately, and homogenate was prepared for Western analysis of TNFR1. QUE is quercetin and BW is body weight. DL, DLT25, DLT50,

and DLT75 represent Dalton's lymphoma-bearing group and Dalton's lymphoma-bearing group treated with 25, 50, and 75 mg QUE/kg BW respectively. One-way analysis of variance (ANOVA) followed by Tukey test was used for statistical analysis. Data represent the mean \pm S.E.M. of three independent experiments. ** and *** denotes significant differences at the level of $p < 0.01$ and $p < 0.001$ respectively, between the DL and QUE treated DL groups

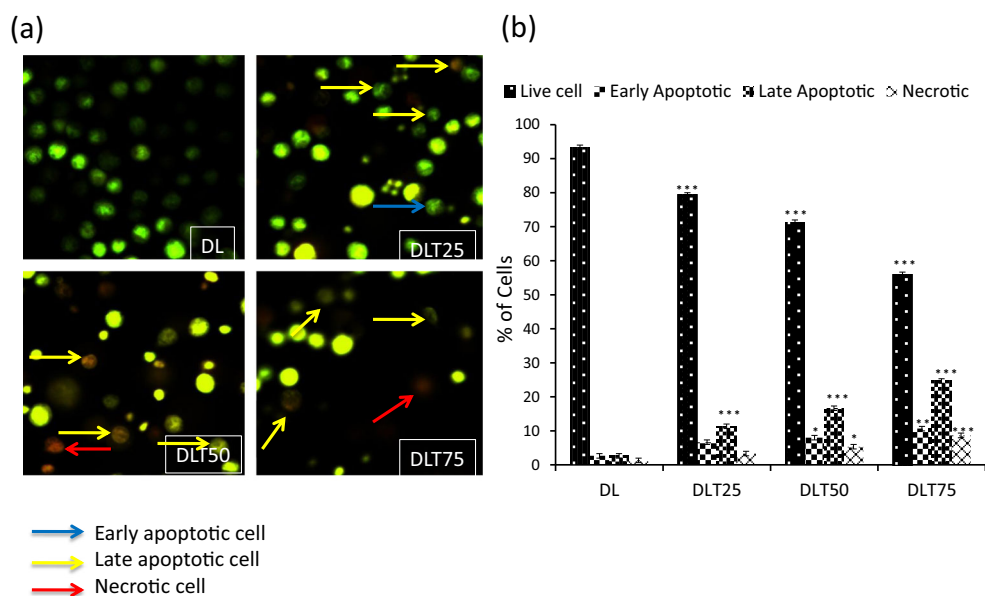


Fig. 6 Apoptosis assay by EB/AO staining. Effect of QUE on apoptosis in ascite cells of lymphoma-bearing mice. **a** Ethidium bromide/Acridine orange staining of DL cells and **b** quantitative analysis of apoptosis. Ascite cells of all six animals of each group were pooled separately for the analysis of apoptosis. QUE is quercetin and BW is body weight. Blue, yellow, and red arrows indicate early apoptotic, late apoptotic, and necrotic cells respectively in Ethidium bromide/Acridine orange staining. DL, DLT25, DLT50, and DLT75 represent Dalton's

lymphoma-bearing group and Dalton's lymphoma-bearing group treated with 25, 50, and 75 mg QUE/kg BW respectively. One-way analysis of variance (ANOVA) followed by Tukey test was used for statistical analysis. Data represent the mean±S.E.M. of three independent experiments. *, **, and *** denote significant differences at the level of $p < 0.05$, $p < 0.01$, and $p < 0.001$ respectively, between the DL and QUE-treated DL groups

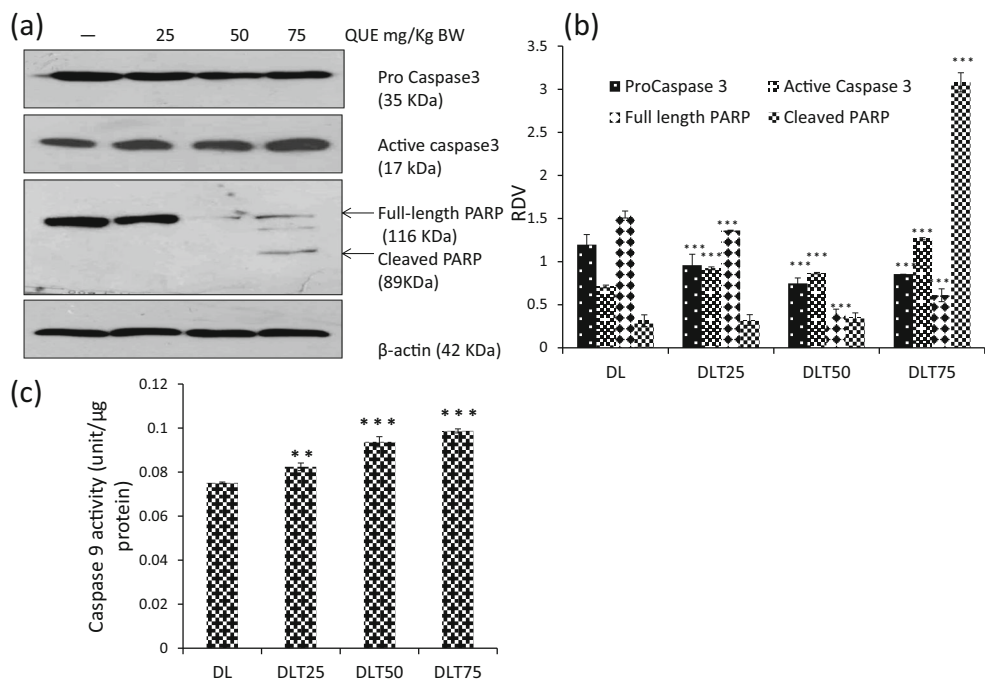


Fig. 7 Level of caspase 3, PARP, and caspase 9 activity. Effect of QUE on protein level of caspase 3, PARP, and caspase 9 activity in ascite cells of lymphoma-bearing mice. **a** Western analysis of caspase 3, PARP, and β -actin. **b** Densitometric scanning of caspase 3 and PARP after normalization with β -actin. **c** Caspase 9 activity. Ascite cells of all six animals of each group were pooled separately, and homogenate was prepared for Western analysis of caspase 3, PARP, and caspase 9 activity. QUE is quercetin and BW is body weight. DL, DLT25, DLT50,

and DLT75 represent Dalton's lymphoma-bearing group and Dalton's lymphoma-bearing group treated with 25, 50, and 75 mg QUE/kg BW respectively. One-way analysis of variance (ANOVA) followed by Tukey test was used for statistical analysis. Data represent the mean±S.E.M. of three independent experiments. ** and *** denotes significant differences at the level of $p < 0.01$ and $p < 0.001$ respectively, between the DL and QUE treated DL groups

Elevated level of caspase 9, 3 and cleaved PARP and morphological assessment support the anti-apoptotic potential of QUE in ascite cells of DL mice.

Effect of QUE on the transcriptional expression of the PKC isoform

The effect of QUE on classical, novel, and atypical PKC signaling was analyzed by mRNA level [Fig. 8]. The treatment of QUE modulates the expression of PKC isozymes in ascite cells of DL mice. QUE significantly downregulates the expression of PKC α approximately by 17, 9, and 25 % with a dose of 25, 50, and 75 mg QUE/kg BW respectively. The expression of PKC β significantly downregulated approximately by 44, 29, and 36 % and upregulated expression of PKC γ approximately by 17, 18, and 23 % with a dose of 25, 50, and 75 mg QUE/kg BW respectively. QUE is found to regulate classical PKC signaling by downregulating the expression of PKC α and PKC β and upregulation of the PKC γ expression. PKC δ , a known pro-apoptotic isozyme, was found to be upregulated by QUE approximately by 74, 62, and 55 % with a dose of 25, 50, and 75 mg QUE/kg BW respectively. Further, PKC η and PKC ϵ expression was

decreased with a dose 75 and 25 mg QUE/kg BW respectively. QUE modulates atypical signaling via downregulation of the expression of PKC ζ , and upregulation of the expression of PKC ι in ascite cells.

Discussion

Deregulated signaling of protein kinase C promotes cancer growth by loss of apoptosis and increased cell proliferation. Oxidative stress modulates PKC activity. QUE in this context may play a key role to overcome oxidative stress in cancer cells. Previously, we have reported that QUE suppresses DL growth via downregulating cell proliferation, energy metabolism, and PI3K/AKT signaling [36]. In the present study, we have demonstrated that QUE may provoke apoptosis via downregulation of ROS and TNFR1 level in DL mice. Initial results show that QUE downregulates the total ROS level in ascite cells progressively with an increase in QUE dose. This reduced ROS level may help the suppression of tumor growth. Further, the total PKC activity was downregulated after QUE treatment. It indicates that QUE reduces the ROS level via downregulating PKC activity. PKC activation is differentially

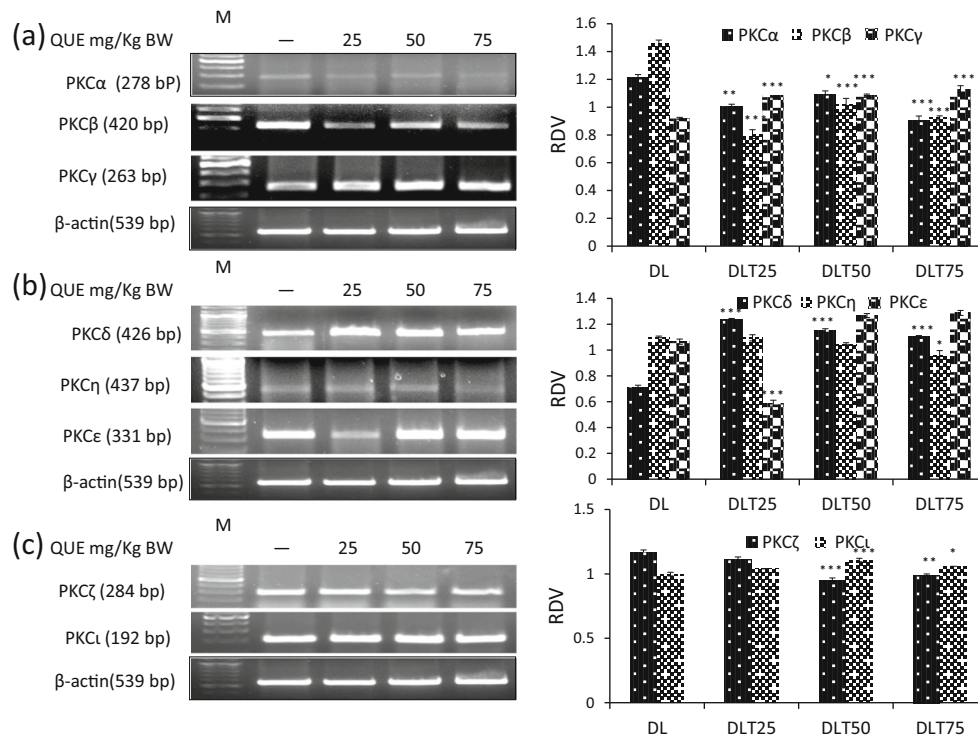


Fig. 8 Expression of PKC isoforms. Effects of QUE on mRNA expression in ascite cells of lymphoma-bearing mice. **a** Expression of classical PKC (PKC α , PKC β , and PKC γ). **b** Expression of novel PKC (PKC δ , PKC η , and PKC ϵ). **c** Expression of atypical PKC (PKC ζ and PKC ι). Ascite cells of all six animals of each group were pooled separately and used for extraction of total RNA. QUE is quercetin, M is 100 bp marker, and BW is body weight. DL, DLT25, DLT50, and DLT75

represent Dalton's lymphoma-bearing group and Dalton's lymphoma-bearing group treated with 25, 50, and 75 mg QUE/kg BW respectively. One-way analysis of variance (ANOVA) followed by Tukey test was used for statistical analysis. Data represent the mean \pm S.E.M. of three independent experiments. *, **, and *** denote significant differences at the level of $p < 0.05$, $p < 0.01$, and $p < 0.001$ respectively, between the DL and QUE-treated DL groups

regulated by cellular oxidants: oxidation at the NH₂-terminal regulatory domain activates PKC, whereas oxidation at the COOH terminal inactivates the PKC [10].

The PKC family consists of multiple isoenzymes with different distribution and functions [46]. PKC α has emerged as an important isoform to promote cell survival. Cellular depletion of PKC α is reported to induce apoptosis [24, 47–50]. Although the mechanism behind PKC α preventing apoptosis is still a matter of debate, Bcl-2 and Raf-1 have been shown to mediate the anti-apoptotic function of AKT in the regulation of PKC α . Reduced activation of AKT and ERK in the PKC α knockdown tumor model suggests that PKC α is an upstream regulator of these critical growth and survival signaling pathways. In an earlier work, we have found that QUE downregulates PI3K/AKT signaling in ascite cells of DL mice [36]. In the present study, a decreased level of PKC α in the total lysate of ascite cells of DL mice after QUE treatment may be due to a reduced level of ROS in ascite cells. The result supports earlier findings showing QUE and other flavonoids to downregulate PKC α or PKC [51–53]. Activated PKC α is translocated from the cytosol to the membrane compartment. Membrane-bound PKC α is associated with activation of the enzyme [22]. A reduced level of PKC α in the membrane indicates inactivation of PKC α by QUE.

Transcriptional gene expression results suggest that QUE suppresses DL cell growth via modulating the conventional, novel, and atypical PKC pathway. Oxidative stress plays an important role to maintain its high proliferation rate in cancerous cells. The expression of PKC α is reduced by QUE treatment in comparison to untreated ascite cells showing its antioxidant property. Overexpression of PKC α is known to suppress apoptosis during oxidative stress by phosphorylating Bcl-2 [54]. An elevated expression of PKC β has been observed in colon cancer development [55]. PKC β phosphorylates AKT at serine 473, consistent with a pro-survival function [56]. Our result of the downregulation of PKC β by QUE treatment supports the earlier report indicating that PKC β promotes cell survival during cancer growth. It has been reported that PKC ι mediates activation of NF-E2-related factor 2 (Nrf2) [57]. Nrf2 acts as transcription factor and regulates the induction of antioxidative proteins. QUE-treated mice show a relative increase in PKC ι expression as compared with untreated DL mice, suggesting that QUE reduces oxidative stress by stimulation of PKC ι expression. Under oxidative stress, the cell stimulates the production of stress-activated proteins that help the cells to survive in the cancer microenvironment. One of these stress-defending proteins is A170 which has a structural domain to interact with PKC ζ [58]. PKC ζ is observed to be reduced with QUE treatment of DL mice. The result is in correlation with ROS by QUE. Reduced oxidative stress by QUE may inhibit cell survival via the PKC ζ pathway. PKC δ is known to be a pro-apoptotic protein. Improved expression of PKC δ , observed by QUE treatment,

shows that QUE contributes in the regression of lymphoma via apoptosis.

TNF-receptor I (TNFR1) is well known to induce apoptosis as well as activate transcription factor NF- κ B with promoting cell survival [33, 59–62]. TNFR1 also activates MAPK, which directly phosphorylates I κ B β kinase (IKK β). Further, TNFR1 promotes breast cancer growth via p42/P44 MAPK, JNK, AKT, and NF- κ B-dependent pathways [63]. TNFR1 follows two different mechanisms to trigger apoptosis [64]. The TNF-stimulated receptor is reported to aggregate and form receptor clustering or “capping,” and then is internalized through clathrin-mediated endocytosis. Cytosolic TNFR1 is assembled with FADD, which in turn recruits caspase 8 and 10 to form the cytosolic complex (complex II). Complex II is temporally and spatially distinct from initial plasma membrane-bound complex I. The assembly of complex II is critically dependent on receptor endocytosis, which is regulated by a cytoplasmic region named TNFR1 internalization domain (TRID) [65]. However, it has recently been suggested that the components of the receptor-associated signaling complex may be released from the receptor to form a secondary cytosolic complex, or complex II. The function of this newly identified complex II is likely to enhance the activation of caspase 8. The formation of complex II does not depend on receptor internalization [60].

Our data reveals that the membranous TNFR1 level is subsequently downregulated on QUE treatment which might be correlated with the inactivation of NF- κ B and reduced survival of cells. Additionally, an increased level of cytosolic TNFR1 on QUE treatment might be due to internalization of TNFR1 which induces apoptosis via caspase-8 activation. Interestingly, QUE downregulates the level of TNFR1 in whole ascite cell lysate. The higher level of TNFR1 in DL cells is in accordance with a previous study which suggested that when NF- κ B is activated by complex I, complex II harbors the caspase-8 inhibitor FLIP and the cell survives. QUE suppresses cell survival by decreasing the level of TNFR1. QUE may reduce cell survival and promotes apoptosis via differential localization of the TNFR1 level in ascite cells of Dalton’s lymphoma-bearing mice. QUE is also reported to promote cell apoptosis via inhibiting the expression of extracellular matrix proteins MMP-9 [66].

Cancerous cells avoid apoptosis or programmed cell death and promote uncontrolled cell proliferation. Therefore, the role of QUE on uncontrolled cell growth of Dalton’s lymphoma cells needs to be defined. Apoptosis is a hallmark of anti-carcinogenesis and caspase as well as PARP are key players in apoptosis [45]. QUE treatment decreased the level of procaspase 3 and increased active caspase 3. An improved activity of caspase 9 was also found on QUE treatment. Caspase 3 is a critical executioner of apoptosis. It is either partially or totally responsible for proteolytic cleavage of poly (ADP-ribose) polymerase (PARP). PARP is a 116-kDa nuclear poly

(ADP-ribose) polymerase involved in DNA repair in response to environmental stress. PARP is cleaved by different caspases *in vitro* and is one of the main cleavage targets of caspase 3 *in vivo*. Cleavage of PARP facilitates cellular disassembly and serves as a marker of cells undergoing apoptosis. A decreased level of full-length PARP is observed with all doses of QUE. However, the cleavage of PARP could be detected with 75 mg QUE/kg BW.

Further, confirmation of apoptosis was supported by nuclear condensation. Different apoptotic stimuli such as TNF- α and UV radiation induce cleavage of PKC δ , resulting in the generation of a constitutively active catalytic fragment which has been implicated in its apoptotic function. PKC δ has been reported to cause DNA-damage-induced apoptosis in HeLa cells [67]. Caspase-3-dependent cleavage of PKC δ induces apoptosis in different cellular system [26, 28, 44]. QUE upregulates the level of CF of PKC δ in DL mice as well as promotes caspase 3 activity which suggests that QUE modulates caspase-3-dependant PKC δ activity leading to apoptosis. PKC δ null mice develop normally, suggesting that PKC δ is not required for normal cell proliferation. Recently, PKC δ was considered as a major PKC isoform responsible for inhibition of PI3K [68]. Our results indicate that QUE suppresses uncontrolled cell growth of DL mice via improving apoptotic potential.

The overall results show that QUE suppresses cell proliferation and survival and induces apoptosis by modulating both intrinsic and extrinsic pathways via ROS-mediated PKC signaling. The findings may provide a base for using QUE as a chemotherapeutic drug in the prevention of cancer.

Acknowledgments The research was supported by University Grants Commission (UGC), India. AKM thanks the Council of Scientific and Industrial Research (CSIR), India, for Senior Research Fellowship (CSIR Award No. File No: 09/013(0338)/2010-EMR-I).

Conflicts of interest None

References

- Nogueira V, Hay N. Molecular pathways: reactive oxygen species homeostasis in cancer cells and implications for cancer therapy. *Clin Cancer Res*. 2013;19:4309–14.
- Sosa V, Moliné T, Somoza R, Paciucci R, Kondoh H, LLeonart ME. Oxidative stress and cancer: an overview. *Ageing Res Rev*. 2013;12:376–90.
- Valko M, Rhodes CJ, Moncol J, Izakovic M, Mazur M. Free radicals, metals and antioxidants in oxidative stress-induced cancer. *Chem Biol Interact*. 2006;160:1–40.
- Ivanova D, Bakalova RLD, et al. The impact of reactive oxygen species. *Clin Adv Med Exp*. 2013;22:899–908.
- Weinberg F, Chandel NS. Reactive oxygen species-dependent signaling regulates cancer. *Cell Mol Life Sci*. 2009;66:3663–73.
- Naka K, Muraguchi T, Hoshii T, Hirao A. Regulation of reactive oxygen species and genomic stability in hematopoietic stem cells. *Antioxid Redox Signal*. 2008;10:1883–94.
- Trachootham D, Alexandre J, Huang P. Targeting cancer cells by ROS-mediated mechanisms: a radical therapeutic approach. *Nat Rev Drug Discov*. 2009;8:579–91.
- Coleman WB, Tsongalis GJ. Molecular mechanisms of human carcinogenesis. Cancer: cell structures, carcinogens and genomic instability. *EXS*. 2006;96:321–49.
- Wu WS. The signaling mechanism of ROS in tumor progression. *Cancer Metastasis Rev*. 2006;25:695–705.
- Gopalakrishna R, Gundimeda U. Antioxidant regulation of protein kinase C in cancer prevention. *J Nutr*. 2002;132:3819–23.
- Trachootham D, Lu W, Ogasawara MA, Nilsa RDV, Huang P. Redox regulation of cell survival. *Antioxid Redox Signal*. 2008;10:1343–74.
- Zhou F, Shen Q, Claret FX. Novel roles of reactive oxygen species in the pathogenesis of acute myeloid leukemia. *J Leukoc Biol*. 2013;94:423–9.
- Saeidnia S, Abdollahi M. Antioxidants: friends or foe in prevention or treatment of cancer: the debate of the century. *Toxicol Appl Pharmacol*. 2013;271:49–63.
- Samoylenko A, Hossain J, Mennerich D, Kellokumpu S, Hiltunen JK, Kietzmann T. Nutritional countermeasures targeting reactive oxygen species in cancer: from mechanisms to biomarkers and clinical evidence. *Antioxid Redox Signal*. 2013;19:2157–96.
- Glasauer A, Chandel NS. Targeting antioxidants for cancer therapy. *Biochem Pharmacol*. 2014;92:90–101.
- Hu CT, Wu JR, Cheng CC, Wang S, Wang HT, Lee MC, et al. Reactive oxygen species-mediated PKC and integrin signaling promotes tumor progression of human hepatoma HepG2. *Clin Exp Metastasis*. 2011;28:851–63.
- Aspects D, Giorgi C, Agnoletto C, Baldini C, Bononi A, Bonora M, et al. Redox control of protein kinase C : cell-and disease-specific aspects. *Antioxid Redox Signal*. 2010;13:1051–85.
- Paulsen CE, Carroll KS. Orchestrating redox signaling networks through regulatory cysteine switches. *ACS Chem Biol*. 2010;5:47–62.
- Frey RS, Gao X, Javaid K, Siddiqui SS, Rahman A, Malik AB. Phosphatidylinositol 3-kinase gamma signaling through protein kinase Czeta induces NADPH oxidase-mediated oxidant generation and NF-kappaB activation in endothelial cells. *J Biol Chem*. 2006;281:16128–38.
- Talior I, Tennenbaum T, Kuroki T, Eldar-Finkelman H. PKC-delta-dependent activation of oxidative stress in adipocytes of obese and insulin-resistant mice: role for NADPH oxidase. *Am J Physiol Endocrinol Metab*. 2005;288:405–11.
- Caino MC, Meshki J, Kazanietz MG. Hallmarks for senescence in carcinogenesis: novel signaling players. *Apoptosis*. 2009;14:392–408.
- Mishra S, Vinayak M. Anti-carcinogenic action of ellagic acid mediated via modulation of oxidative stress regulated genes in Dalton lymphoma bearing mice. *Leuk Lymphoma*. 2011;52:2155–61.
- Lee SK, Shehzad A, Jung JC, Sonn JK, Lee JT, Park JW, et al. Protein kinase C α protects against multidrug resistance in human colon cancer cells. *Mol Cells*. 2012;34:61–9.
- Konopatskaya O, Poole AW. Protein kinase C α : disease regulator and therapeutic target. *Trends Pharmacol Sci*. 2010;31:8–14.
- Wu TT, Hsieh YH, Hsieh YS, Liu JY. Reduction of PKC alpha decreases cell proliferation, migration, and invasion of human malignant hepatocellular carcinoma. *J Cell Biochem*. 2008;103:9–20.
- Zhao M, Xia L, Chen GQ. Protein kinase c δ in apoptosis: a brief overview. *Arch Immunol Ther Exp*. 2012;60:361–72.
- Reyland ME. Protein kinase C δ and apoptosis. *Biochem Soc Trans*. 2007;35:1001–4.

28. Ghayur BT, Hugunin M, Talanian RV, Ratnofsky S, Quinlan C, Emoto Y, et al. Proteolytic activation of protein kinase C δ by an ICE/CED 3-like protease induces characteristics of apoptosis. *J Exp Med*. 1996;184:2399–404.
29. Kanthasamy AG, Kitazawa M, Yang Y, Anantharam V, Kanthasamy A. Environmental neurotoxin dieldrin induces apoptosis via caspase-3-dependent proteolytic activation of protein kinase C delta (PKCdelta): implications for neurodegeneration in Parkinson's disease. *Mol Brain*. 2008;12:1–15. doi:10.1186/1756-6606-1-12.
30. Oh J, Chun K, Joo S, Oh Y, Lee S. Caspase-3-dependent protein kinase C delta activity is required for the progression of Ginsenoside-Rh2-induced apoptosis in SK-HEP-1 cells. *Cancer Lett*. 2005;230:228–38.
31. Thorburn A. Death receptor-induced cell killing. *Cell Signal*. 2004;16:139–44.
32. Pobeziinskaya YL, Liu Z. The role of TRADD in death receptor signaling. *Cell Cycle*. 2012;11:871–6.
33. Baud V, Karin M. Signal transduction by tumor necrosis factor and its relatives. *Trends Cell Biol*. 2001;11:372–7.
34. Tracey D, Klareskog L, Sasso EH, Salfeld JG, Tak PP. Tumor necrosis factor antagonist mechanisms of action: a comprehensive review. *Pharmacol Ther*. 2008;117:244–79.
35. Wajant H, Scheurich P. TNFR1-induced activation of the classical NF- κ B pathway. *FEBS J*. 2011;278:862–76.
36. Maurya AK and Vinayak M. Quercetin regresses Dalton's lymphoma growth via suppression of PI3K/AKT signaling leading to up regulation of p53 and decrease in energy metabolism. *Nutr Cancer*. 2014;67:354–63.
37. Hayashi A. Effects of daily oral administration of quercetin chalcone and modified citrus pectin on implanted colon-25 tumor growth in Balb-c mice. *Altern Med Rev*. 2006;5:546–52.
38. Goldie H, Dingman FM. Growth characteristics of free tumor cells transferred serially in the peritoneal fluid of the mouse. *Cancer Res*. 1951;11:73–80.
39. Aita K, Irie H, Tanuma Y, Toida S, Okuma Y, Mori S, et al. Apoptosis in murine lymphoid organs following intraperitoneal administration of dimethyl sulfoxide (DMSO). *Exp Mol Pathol*. 2005;79:265–71.
40. Chen N, Ma WY, Huang C, Dong Z. Translocation of protein kinase C and protein kinase C to membrane is required for ultraviolet B-induced activation of mitogen-activated protein kinases and apoptosis. *J Biol Chem*. 1999;274:15389–94.
41. Qian W, Nishikawa M, Haque AM, Hirose M, Mashimo M, Sato E, et al. Mitochondrial density determines the cellular sensitivity to cisplatin-induced cell death. *Am J Physiol Cell Physiol*. 2005;289:C1466–75.
42. Ribble D, Goldstein NB, Norris DA, Shellman YG. A simple technique for quantifying apoptosis in 96-well plates. *BMC Biotechnol*. 2005;7:1–7.
43. Das L, Vinayak M. Long term effect of curcumin in regulation of glycolytic pathway and angiogenesis via modulation of stress activated genes in prevention of cancer. *PLoS ONE*. 2014;9:1–12.
44. Mishra S, Vinayak M. Ellagic acid induces novel and atypical PKC isoforms and promotes caspase-3 dependent apoptosis by blocking energy metabolism. *Nutr Cancer*. 2014;66:675–81.
45. Elmore S. Apoptosis: a review of programmed cell death. *Toxicol Pathol*. 2007;35:495–516.
46. Gutcher I, Webb PR, Anderson NG. The isoform-specific regulation of apoptosis by protein kinase C. *Cell Mol Life Sci*. 2003;60:1061–70.
47. Mauro A. PKCalpha-mediated ERK, JNK and p38 activation regulates the myogenic program in human rhabdomyosarcoma cells. *J Cell Sci*. 2002;115:3587–99.
48. Martiny-Baron G, Fabbro D. Classical PKC isoforms in cancer. *Pharmacol Res*. 2007;55:477–86.
49. Lahn M, Sundell K, Gleave M, Ladan F, Su C, Li S, et al. Protein kinase C- α in prostate cancer. *BJU Int*. 2004;93:1076–81.
50. Zhang XM, Chen J, Xia YG, Xu Q. Apoptosis of murine melanoma B16-BL6 cells induced by quercetin targeting mitochondria, inhibiting expression of PKC-alpha and translocating PKC-delta. *Cancer Chemother Pharmacol*. 2005;55:251–62.
51. Gamet-Payrastrre L, Manenti S, Gratacap M-P, Tulliez J, Chap H, Payrastrre B. Flavonoids and the inhibition of PKC and PI 3-kinase. *Gen Pharmacol Vasc Syst*. 1999;32:279–86.
52. Granado-serrano AB, Martín MA, Bravo L, Goya L. Time-course regulation of quercetin on cell survival / proliferation pathways in human hepatoma cells. *Mol Nutr Food Res*. 2008;52:457–64.
53. Wu CH, Wu CF, Huang HW, Jao YC, Yen GC. Naturally occurring flavonoids attenuate high glucose-induced expression of proinflammatory cytokines in human monocytic THP-1 cells. *Mol Nutr Food Res*. 2009;53:984–95.
54. Ruvolo PP, Deng X, Carr BK, May WS, Biol WSJ, Reh H. A functional role for mitochondrial protein kinase C α in Bcl2 phosphorylation and suppression of apoptosis. *J Biol Chem*. 1998;273:25436–42.
55. Popla YG, Murray NR, Velasco MA, Gatalica Z, Fields AP. Elevated protein kinase C β II is an early promotive event in colon carcinogenesis. *Cancer Res*. 2001;2:1375–81.
56. Kawakami Y, Nishimoto H, Kitaura J, Maeda-Yamamoto M, Kato RM, Littman DR, et al. Protein kinase C betaII regulates Akt phosphorylation on Ser-473 in a cell type- and stimulus-specific fashion. *J Biol Chem*. 2004;279:47720–5.
57. Numazawa S, Ishikawa M, Yoshida A, Tanaka S, Yoshida T. Atypical protein kinase C mediates activation of NF-E2-related factor 2 in response to oxidative stress. *Am J Physiol Cell Physiol*. 2003;285:334–42.
58. Kim JH, Kim JH, Ohba M, Suh PG, Ryu SH. Novel functions of the phospholipase D2-Phox homology domain in protein kinase Czeta activation. *Mol Cell Biol*. 2005;25:3194–208.
59. Chen G, Goeddel DV. TNF-R1 signaling: a beautiful pathway. *Science*. 2002;296:1634–5.
60. Micheau O, Boveresses C, Epalinges C. Induction of TNF receptor I-mediated apoptosis via two sequential signaling complexes. *Cell*. 2003;114:181–90.
61. Liu Z, Hsu H, Goeddel DV, Karin M. Dissection of TNF receptor 1 effector functions: JNK activation is not linked to apoptosis while NF- κ B activation prevents cell death. *Cell*. 1996;87:565–76.
62. D'Alessio A, Kluger MS, Li JH, Al-Lamki R, Bradley JR, Pober JS. Targeting of tumor necrosis factor receptor 1 to low density plasma membrane domains in human endothelial cells. *J Biol Chem*. 2010;285:23868–79.
63. Rivas MA, Carnevale RP, Proietti CJ, Rosembli C, et al. TNF α acting on TNFR1 promotes breast cancer growth via p42/p44 MAPK, JNK, Akt and NF- κ B-dependant pathways. *Exp Cell Res*. 2008;314:509–29.
64. Guicciardi ME, Gores GJ. Life and death by death receptors. *FASEB J*. 2009;23:1625–37.
65. Brachert WS, Tchikov V, Neumeyer J, Jakob M, Morbach SW, Feindt JF, et al. Compartmentalization of TNF receptor 1 signaling: internalized TNF receptors as death signaling vesicles. *Immunity*. 2004;21:415–28.
66. Pan HC, Jiang Q, Yu Y, Mei JP, Cui YK, Zhao WJ. Quercetin promotes cell apoptosis and inhibits the expression of MMP-9 and fibronectin via the AKT and ERK signalling pathways in human glioma cells. *Neurochem Int*. 2015;80:60–71.
67. Basu A, Woolard MD, Johnson CL. Involvement of protein kinase C-delta in DNA damage-induced apoptosis. *Cell Death Differ*. 2001;8:899–908.
68. Hazeki K, Inoue K, Nigorikawa K, Hazeki O. Negative regulation of class IA phosphoinositide 3-kinase by protein kinase Cdelta limits Fcgamma receptor-mediated phagocytosis in macrophages. *J Biochem*. 2009;145:87–94.